NEOPLASIA
www.neoplasia.com
Volume 22 Number 1 January 2020 pp. 1–9

Liver X Receptor Agonism Sensitizes a Subset of Hepatocellular Carcinoma to Sorafenib by Dual-Inhibiting MET and EGFR

Weiqing Shao[a,1]; Wenwei Zhu[a,1]; Jing Lin[a,1]; Mengjun Luo[b]; Zhifei Lin[a]; Lu Lu[a]; Huliang Jia[a]; Lunxiu Qin[a,c,*]; Ming Lu[a,*]; Jinhong Chen[a,*]

[a]Department of General Surgery, Huashan Hospital, Fudan University, 12 Urumqi Road (M), Shanghai 200040, China; [b]Key Laboratory of Medical Molecular Virology (MOE & MOH), Institutes of Biomedical Sciences, Fudan University, 138 Yi Xue Yuan Road, Shanghai 200032, China; [c]Institutes of Biomedical Sciences, Fudan University, 138 Yi Xue Yuan Road, Shanghai 200032, China Address all Correspondence to: Lunxiu Qin, or Ming Lu or Jinhong Chen, Department of General Surgery, Huashan Hospital, Fudan University, 12 Urumqi Road (M), Shanghai 200040, China.

Abstract

Sorafenib is the first approved systemic therapy for advanced hepatocellular carcinoma (HCC) and is the first-line choice in clinic. Sustained activation of receptor tyrosine kinases (RTKs) is associated with low efficacy of sorafenib in HCC. Activation of liver X receptor (LXR) has been reported to inhibit some RTKs. In this study, we found that the LXR agonist enhanced the anti-tumor activity of sorafenib in a subset of HCC cells with high LXR-β/α gene expression ratio. Mechanically, the activation of LXR suppressed sorafenib dependent recruitment of MET and epidermal growth factor receptor (EGFR) in lipid rafts through cholesterol efflux. Our findings imply that LXR agonist can serve as a potential sensitizer to enhance the anti-tumor effect of sorafenib.

Neoplastic (2019) 22 1–9

Introduction

Hepatocellular carcinoma (HCC) is one of the leading causes of cancer-related death worldwide [1]. Sorafenib, a tyrosine kinase inhibitor (TKI), is the first approved systemic therapy for advanced HCC and is the first-line choice in clinic. However, only a small part of HCC patients are sensitive to sorafenib [2,3]. Combination of sorafenib with other drugs or compounds maybe a way to enhance the sensitivity of sorafenib. Recent studies have shown that aberrant activations of several receptor tyrosine kinases (RTKs) and their downstream pathways are strongly correlated with the disrupted efficacy of sorafenib [4–7]. Among these kinases, MET and epidermal growth factor receptor (EGFR) are presumed to be the most promising targets, as strategies combining MET or EGFR inhibitors with sorafenib have shown benefits in preclinical models [8–10]. However, compensatory activation of untargeted kinases and unpredictable crosstalk between them have limited further progression of combination strategy [11]. All these observations highlight the necessity of elucidating the mechanism behind over-activation of RTKs and seeking solutions that can block multiple RTKs.

Liver X receptor (LXR) is a member of the nuclear receptor (NR) superfamily of ligand-dependent transcription factors, which has a key function in regulating cholesterol homeostasis [12]. Recently, accumulating evidences have demonstrated that LXR is involved in a variety of malignancies and is considered highly druggable therapeutic targets [13–17]. Agonists of LXR have shown broad-spectrum anti-tumor effects in various cancers by inhibiting RTKs, such as EGFR and vascular endothelial growth factor receptor 2 (VEGFR2) [18,19]. However, the effect of LXR activation on other RTKs like MET and the mechanism by which LXR inhibits these kinases remain unknown. RTKs and other growth factors depend on complete and stable cytomembrane to promote growth. Since LXRs can regulate membrane composition and function by modulating cholesterol and other lipid metabolism, we suggest that LXRs can inhibit multiple RTKs and the inhibition is related to cholesterol metabolism [19–21]. More recently, increasing malignancies depend heavily on cellular cholesterol to support their growth and metastasis, and LXR agonists have shown remarkable anti-cancer effects in these tumors by reducing cellular cholesterol [22,23]. But whether cholesterol metabolism plays a central role in the anti-tumor effects of LXR agonists requires further investigations. And the effect of LXR-mediated inhibition of RTKs on sorafenib's efficacy remains to be elucidated.

In this study, we determine the effects of the combination of an LXR agonist, T0901317, and sorafenib on the growth of a subset of HCC cells and their xenografts, and further reveal the underlying mechanism.

Received 10 May 2019; received in revised form 8 August 2019; accepted 12 August 2019

https://doi.org/10.1016/j.neo.2019.08.002

[1] These authors contributed equally to this work.
e-mail addresses: qinlx@fudan.edu.cn (L. Qin), luming@huashan.org.cn (M. Lu), jinhongch@hotmail.com (J. Chen)

Materials and Methods

Reagents Sorafenib (multikinase inhibitor), T0901317 (LXR pan-agonist), GW3965 (LXR pan-agonist), PF-04217903 (ATP-competitive Met inhibitor), Gefitinib (EGFR-tyrosine kinase inhibitor), MK-2206 (Akt1/2/3 inhibitor), SCH772984 (ERK1/2 inhibitor), and SB202190 (p38 MAPK Inhibitor) were purchased from Selleck Chemicals (Houston, TX, US). Antibodies against LXRα and LXRβ were purchased from Abcam cooperation (Cambridge, UK). All other antibodies were purchased from Cell Signaling Technology (Danvers, MA, USA). Puromycin and TRIzol reagent were purchased from Thermo Fisher Scientific (Grand Island, NY, USA). Cell Counting Kit-8 (CCK-8) was purchased from Dojindo Laboratories (Mashikimachi, kamimashiki gun Kumamoto, JAPAN). PI/RNase Staining Buffer and FITC Annexin V Apoptosis Detection Kit were purchased from BD Biosciences (San Diego, CA, USA). Cholesterol Assay Kit was purchased from Invitrogen (San Diego, CA, USA). BCA Protein Assay Reagent was purchased from Beyotime Biotechnology (Shanghai, China).

Cell Culture

Human HCC cell lines MHCC97H, HCCLM3 were obtained from Liver Cancer Institute, Fudan University, Shanghai, China. Other HCC cell lines Hep3B and HepG2 were purchased from Cell Resources Center, Chinese Academy of Sciences, Shanghai, China. All cell lines were cultured in high-glucose DMEM supplemented with 10% FBS in an atmosphere of 5% CO_2 at 37 C.

Clinical Specimens

HCC tumor and non-tumor specimens were collected during surgical resection. This study contains 36 HCC patients. None of the patients received any preoperative cancer treatment. Use of HCC specimens was approved by the Ethics Committee of Fudan University.

Growth Assay

Cell proliferation was counted with a CCK-8 assay following the manufacturer's instructions. Briefly, 5 10^3 cells were seeded in triplicate in 96-well plates and incubated in the presence of T0901317, GW3965, or T0901317 with sorafenib at indicated concentrations for 72 h. Then viable cells were counted by detecting the absorbance at OD 450 nm.

Flow Cytometry Assay

For cell cycle analysis, after treatment with DMSO, T0901317 (1 M), sorafenib (3 M) or combination therapy for 72 h, MHCC97H cells were harvested and fixed and stained with PI/RNase Staining Buffer for 15 min at room temperature before analysis. For apoptosis analysis, cells were harvested and resuspended in 1 Binding Buffer, and stained with PI and FITC Annexin V at room temperature for 15 min before analysis. Data were acquired using a BD FACSCalibur and analyzed by CellQuest software.

Cholesterol Assay

Cholesterol was extracted using chloroform/methanol (2:1) and quantified by Cholesterol Assay Kit following the manufacturer's instructions. After homogenization and spinning, the organic phase was dried and suspended in a reaction mix containing HRP, cholesterol oxidase, and cholesterol esterase. Absorbance at 590 nm was finally measured in a microplate reader.

Lipid Rafts Extraction

Membrane lipid rafts were isolated by ultracentrifugation on sucrose gradients. In general, after treatment with DMSO, T0901317 (1 M), sorafenib (3 M) or combination therapy for 72 h, MHCC97H cells were harvested and resuspended in 0.5 M Na_2CO_3. A discontinuous sucrose gradient of 40%, 35%, 22%, and 5% sucrose were formed. Tubes were subjected to ultracentrifugation at 200000 g for 20 h in Beckman Coulter Optima LE-80 K swinging rotor SW 40Ti (Beckman) at 4 C. 24 fractions were collected from the top of the gradient. Samples were then subjected to western blot analysis.

Immunohistochemistry

Immunohistochemistry staining of paraffin sections was performed using a two-step protocol with Novolink Polymer Detection System (NovoLink. TM. Detection System, Leica, UK) and the GTVision II Detection Kit (Gene Tech, Shanghai, China). After antigen retrieval, the slices were incubated with the primary antibody overnight at 4 C, followed by incubation with the secondary antibody at 37 C for 30 min. The sections were stained with DAB and counterstained with hematoxylin (Dako, Glostrup, Denmark), dehydrated in ethanol, mounted in dimethyl benzene, and placed under a coverslip.

Western Blot

Cells were harvested in 1x sample buffer, and then boiled for 15 min. The protein concentration was quantified using BCA protein assay reagent. All proteins were separated on 8–12% SDS-PAGE. GAPDH or β-actin was used as control.

Quantitative Real-Time PCR

Total RNA was isolated using the TRIzol Reagent following the manufacturer's protocol. Reverse transcription was performed with PrimeScript RT Master Mix (Takara Bio). Real-time PCR was performed on a 7900HT Fast Real-Time PCR System (Applied Biosystems) using the PrimeSTAR HS DNA Polymerase (Takara Bio). The primers used for amplification of human genes were shown in supplementary materials (Table S1).

Lentiviral Transduction

MHCC97H cells were seeded at a density of 5 10^5 cells/well in 6-well plates and incubated until they reached 50% confluence. Then cells were infected with lentiviral media containing shRNA for LXRα (shLXRα), LXRβ (shLXRβ) and an empty vector as a negative control (shCTRL). Lentiviral selection was performed by culturing the cells in the presence of 3 g/ml of puromycin for 1 week. The shRNA sequences were shown in supplementary materials (Table S2).

Animal Experiments

Male, 4-week-old BALBc nu/nu mice were obtained from Shanghai Laboratory Animal Center, Chinese Academy of Science. All mice were bred in laminar flow cabinets under specific pathogen-free conditions. The experimental protocol was approved by the Shanghai Medical Experimental Animal Care Committee. MHCC97H cells (1 10 [7]) were subcutaneously inoculated into the right flanks of the nude mice. When palpable tumors were formed, mice were randomly assigned to 4 groups (n = 6 for each group), which received a daily oral dose of PBS (control group), 30 mg/kg sorafenib, 10 mg/kg T0901317, or combination ther-

apy for 3 weeks, and tumor samples were then extracted for further analysis. T0901317 was dissolved in Cremophor EL, and sorafenib was in Cremophor EL/ethanol/water (12.5:12.5:75) mixture.

Data Analysis

Data are presented as the mean SEM of three experiments or are representative of experiments repeated at least three times. The data were analyzed using student's T test or Mann–Whitney's test with significance determined as $P < .05$.

Results

LXR Agonist Enhances the Anti-Tumor Effect of Sorafenib in a Subset of HCC Cells

LXR is a key regulator of cholesterol homeostasis and has broad anti-tumor effects *via* inhibition of multiple RTKs [12,24,25]. We first examined the effect of an LXR agonist, T0901317, on proliferation of four human HCC cells, MHCC97H, HCCLM3, Hep3B, and HepG2, and found that T0901317 treatment had no significant effect on cell proliferation of these cells (Fig. 1*A*). We also used another LXR agonist, GW3965, and got similar results (Fig. 1*B*), therefore, T0901317 was used in the following experiments. To determine the effect of T0901317 on the sensitivity of HCC cells to sorafenib, we treated four HCC cells above with combination of sorafenib and T0901317, and found that T0901317 treatment enhanced the suppression effect of sorafenib on the growth of MHCC97H and HCCLM3 cells, but not in Hep3B and HepG2 cells (Fig. 1*C*). Similar discrepancies in the response to combination therapy were also observed between MHCC97L and Huh7 cells (Fig. S1, *A* and *B*). To further confirm the enhancement of LXR agonist on sorafenib's efficacy, we combined GW3965 with sorafenib in MHCC97H cells, and found similar results (Fig. S1*C*). Moreover, sorafenib also improved the anti-proliferation effect of T0901317 in MHCC97H cells (Fig. S1*D*). Combination index (CI) was used to evaluate the effect of combination therapy [26]. CI = 1 indicates additive effect, CI < 1 represents synergism, and CI > 1 means antagonism. To further confirm the above findings, we calculated CI of each cell and found synergism in MHCC97H and HCCLM3 cells (Table 1). These results indicate that T0901317 enhances the anti-tumor effect of sorafenib in a subset of HCC cells.

High LXR-β/α Expression Ratio is Responsible for LXR Agonist-Mediated Enhancement of Anti-Tumor Activity of Sorafenib

To identify the LXR isoform that is responsible for the synergistic effect of LXR agonist and sorafenib, we first examined the expression levels of LXRα and LXRβ in four HCC cells. High LXR-β/α gene expression ratio was detected in MHCC97H and HCCLM3 cells (Fig. 2*A*). We then conducted growth assays in MHCC97H-shLXRα and MHCC97H-shLXRβ cells. Efficiency of knockdown was confirmed by western blot (Fig. 2*B*). Agonism of LXR was proved by detecting mRNA level of cytochrome P450 family 7 subfamily A member 1 (CYP7A1), a canonical

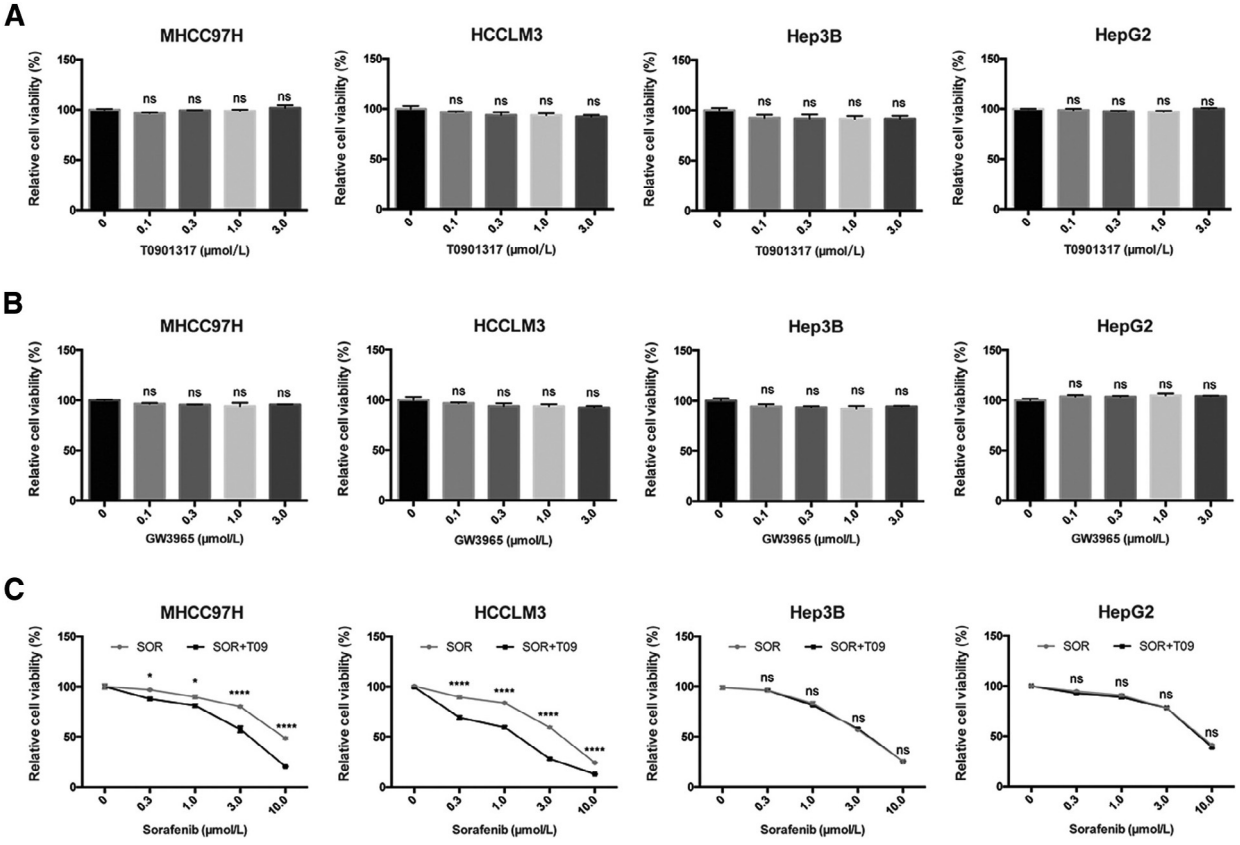

Fig. 1. Anti-proliferative effect of LXR agonists with or without sorafenib in human HCC cells. (A) Effects of T0901317 (T09) on *in vitro* cytotoxicity in MHCC97H, HCCLM3, Hep3B, and HepG2 cells. Cells were incubated in T09 at indicated concentrations for 72 h, then relative viabilities were determined by CCK8 assays. (B) Cells were incubated in GW3965 (GW) at indicated concentrations for 72 h before CCK8 assays. (C) Cells were incubated in sorafenib (SOR) with/without T09 (1 M) for 72 h before detection. N 3, *$P < .05$, ****$P < .0001$.

target gene of LXR (Fig. S2) [27]. The results showed that knockdown of LXRβ rather than LXRα significantly diminished the synergistic effect (Fig. 2, *C–E*), indicating that high LXR-β/α expression ratio is responsible for T0901317-mediated enhancement of anti-tumor activity of sorafenib. To further confirm the role of high LXR-β/α expression ratio in the synergism, we increased the ratio by overexpressing LXRβ in Hep3B cells (Fig. 2*F*). Synergistic effects were observed in Hep3B-LXRβ cells, which verified the necessity of high LXR-β/α expression ratio in the synergism (Fig. 2, *G* and *H*). Moreover, a significant correlation between high LXRβ expression and high tumor grades or poor survival of HCC patient could be observed by using TCGA database (Fig. S3) [28]. Together, these results indicate that high LXR-β/α expression ratio is responsible for LXR agonist-mediated enhancement of anti-tumor activity of sorafenib.

LXR Agonist Enhances the Anti-Tumor Effect of Sorafenib by the Dual Blockade of MET and EGFR

Previous studies have showed that LXR agonists suppressed tumor growth mainly by inducing pro-apoptotic effect or cell cycle arrest [29]. However, we did not observe such effects of LXR agonist on apoptosis or cell cycle arrest in our experiment (Fig. S4). Over-activation of RTKs is thought to be involved in impaired efficacy of sorafenib in HCC [30,31]. We found that the expression of MET and EGFR as well as the IC_{50} value of sorafenib were much higher in MHCC97H and HCCLM3 cells than that in Hep3B and HepG2 cells (Fig. S5). LXR activation suppressed both MET and EGFR and their phosphorylation, and therefore inhibited the downstream pathways alone or with sorafenib in MHCC97H cells (Fig. 3, *A–C*). To confirm the role of MET and EGFR pathways in regulating the efficacy of sorafenib, we then examined the effect of inhibitors of MET and EGFR pathways combined with sorafenib on cell growth in MHCC97H cells. The results showed that inhibition of MET, EGFR, Akt and ERK enhanced the anti-proliferation effect of sorafenib (Fig. 3, *D–H*). Moreover, we found that inhibition of both RTKs and their phosphorylated forms was diminished in MHCC97H-shLXRβ cells comparing with MHCC97H-shCTRL or MHCC97H-shLXRα cells (Fig. 3*I*). These results demonstrate that LXR agonist enhances the anti-tumor effect of sorafenib by dual blockade of MET and EGFR.

LXR agonist suppresses recruitment of MET and EGFR in lipid rafts by promoting cholesterol efflux.

Given that LXR is a core regulator of cholesterol homeostasis, we next investigated the role of cholesterol metabolism in LXR-mediated RTK suppression in HCC. We first measured free and total cholesterol levels of MHCC97H cells in each group, and found that T0901317 alone or in combination with sorafenib reduced both free and total cholesterol

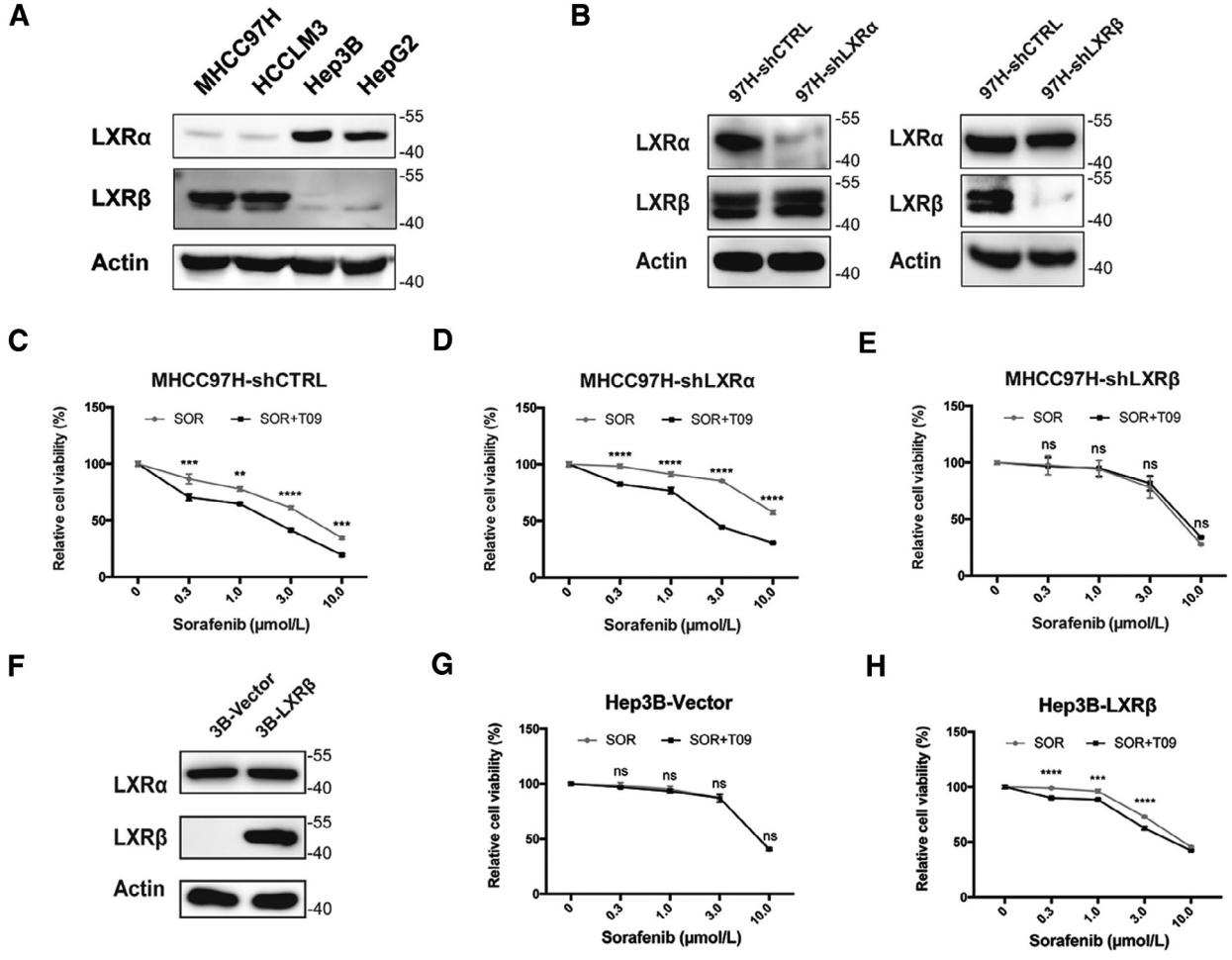

Fig. 2. LXRβ rather than LXRα exerts the synergistic effect. (A) Expression of LXRs in HCC cell lines detected by western blot analysis. (B) Verification of knockdown efficiency of LXRs in MHCC97H cells by western blot. (C-E) Effects of SOR with or without T09 (1 M) on cell viabilities in MHCC97H-shCTRL (C), MHCC97H-shLXRα (D), and MHCC97H-shLXRβ cells (E). (F) Verification of LXRβ overexpression in Hep3B cells by western blot. (G-H) Effects of SOR with or without T09 (1 M) on cell viabilities in Hep3B-Vector (G), and Hep3B-LXRβ cells (H). N 3, $^{**}P < .01$, $^{***}P < .001$, $^{****}P < .0001$.

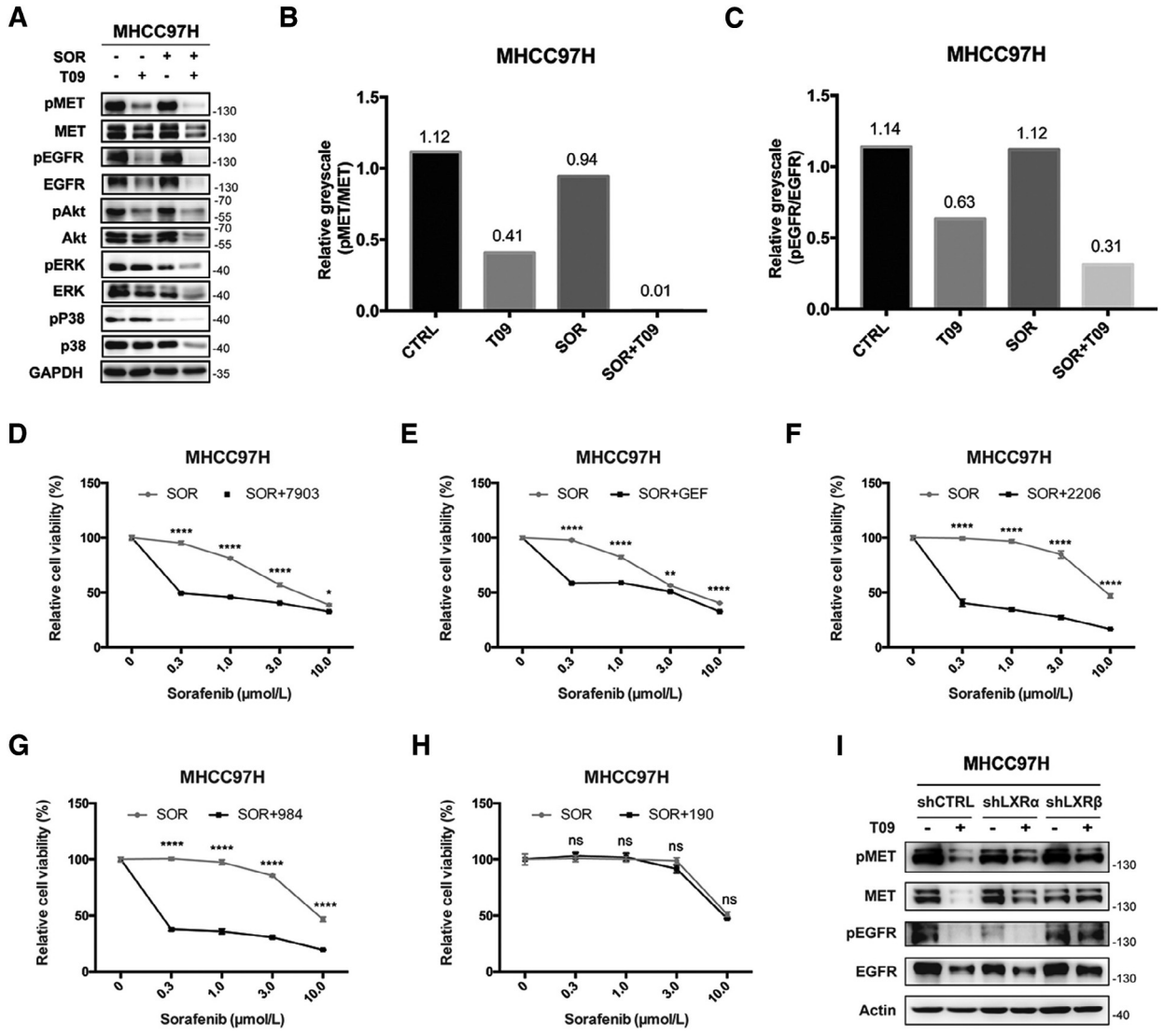

Fig. 3. T0901317 dual-inhibits MET and EGFR. (A) Effects of T09 with or without SOR on MET/EGFR pathways in MHCC97H cells. Cells were incubated in SOR (3 M) with/without T09 (1 M) for 72 h before western blot. (B-C) Quantification of phospho/non-phospho- MET (B) and EGFR (C) in (A). (D-H) Effects of inhibitors targeting MET (D), EGFR (E), Akt (F), ERK (G), and P38 (H) combined with SOR on proliferation of MHCC97H cells. Cells were incubated in SOR with/without PF-04217903 (7903, 10 nM), Gefitinib (GEF, 10 M), MK-2206 (2206, 3 M), SCH772984 (984, 3 M), or SB202190 (190, 3 M) for 72 h before CCK8 assays. (I) Effects of T09 on MET, pMET, EGFR, and pEGFR in MHCC97H-shCTRL, MHCC97H-shLXRα, and MHCC97H-shLXRβ cells. N 3, $^{*}P < .05$, $^{**}P < .01$, $^{****}P < .0001$.

levels (Fig. 4, *A* and *B*). Lipid rafts are reported to play an important role in the regulation of membrane receptors and their downstream pathways [19,20]. RTKs in lipid rafts are functional forms that promote tumor progression. So, we determined protein levels of MET and EGFR in lipid rafts and found that both RTKs were up-regulated after sorafenib treatment and were re-inhibited by T0901317 (Fig. 4*C*). Greyscale analysis of MET and EGFR in Fig. 4*C* confirmed the phenomenon (Fig. 4, *D* and *E*). We also examined the expression of ATP binding cassette subfamily A member 1 (ABCA1), a canonical LXR target gene regulating cholesterol efflux [25], and found that ABCA1 gene expression was up-regulated by treatment of T0901317 (Fig. 4, *F* and *G*), confirming the activation of LXR. Moreover, we found that cholesterol could rescue reduced cell viability in combination group by restoring MET and EGFR expression (Fig. 4, *H* and *I*). Further analysis using paired tumor and non-tumor tissues from 36 patients showed that the cholesterol efflux gene ABCA1 significantly decreased in HCC (Fig. S6*A*), which was consistent with our previous study [32]. Moreover, down-regulation of ABCA1 in HCC patients was also observed by using TCGA data (Fig. S6*B*) [28]. These findings demonstrate that LXR agonist suppresses the recruitment of MET and EGFR in lipid rafts by sorafenib *via* promoting cholesterol efflux.

Table 1. Combination index (CI) of sorafenib and T0901317 in HCC cell lines

Cell lines	Drug doses (SOR:T09)	CI
MHCC97H	3:1	0.37025
HCCLM3	3:1	0.40034
Hep3B	3:1	1.01512
HepG2	3:1	1.44615

Cells were incubated in sorafenib with T0901317 for 72 h. Cell viability was investigated by CCK8 assay. The CI values of four cells analyzed by CompuSyn software are shown.

LXR Agonist Enhances the Anti-Tumor Activity of Sorafenib in Xenograft Model

To determine the efficacy of the combination of sorafenib and T0901317 on HCC tumor growth *in vivo*, we established a MHCC97H xenograft model. The combination of T0901317 treatment significantly enhanced the anti-tumor effects of sorafenib treatment alone (Fig. 5, *A–C*). Also, no obvious body weight loss was observed in mice (Fig. 5*D*). These results were coordinated with our previous findings in cell experiments. Since we had uncovered potential mechanisms underline the synergism between sorafenib and T0901317, we then sought to validate dual-inhibition of MET and EGFR in mouse model. Given that phosphorylated MET and EGFR were main functional forms which promoted cancer progression, we stained pMET and pEGFR by immunohistochemistry (IHC) in tumor tissues of each group. Data showed that T0901317 alone or with sorafenib significantly decreased both pMET and pEGFR, which was consistent with *in vitro* results (Fig. 5*E*). Further quantification of IHC scores of each group also supported these findings (Fig. 5, *F* and *G*). Besides, up-regulation of both pMET and pEGFR were observed in sorafenib group, which indicated compensatory activation. As a multikinase inhibitor, sorafenib was reported to activate various untargeted oncogenic pathways while inhibiting multiple RTKs [33]. And these aberrant activated molecules would provide new targets for combination therapy while counteracting part of sorafenib's anti-tumor effects. Here in our study, compensatorily activated MET and EGFR were re-inhibited by T0901317 in xenograft model. Collectively, our data support the notion that LXR activation enhances the anti-tumor effects of sorafenib in a subset of HCCs.

Discussion

In the present study, we revealed that reduction of cellular cholesterol *via* LXR activation improved sorafenib's efficacy in a subset of HCC cells with a high LXR-β/α gene expression ratio. As is reported elsewhere, the two isoforms of LXR have distinct expression patterns and different functions. LXRβ is ubiquitously expressed at a moderate level in most physiological systems, whereas LXRα expression is mostly restricted to metabolically active tissues like liver [25]. However, high LXRβ expression was found in HCC and correlated with high tumor grades and poor survival (Fig. S3) [28]. Such shift from LXRα to LXRβ may provide new targets for HCC therapy. Besides, despite the highly conserved domains and shared function in cholesterol homeostasis, LXRβ exerts many more non-canonical effects than LXRα. Recent studies have demonstrated that LXRβ could interact directly with ABCA1 to modulate cholesterol efflux [34]. These findings hint that high LXR-β/α gene expression ratio may favor cholesterol efflux under LXR agonism. Other studies have found that

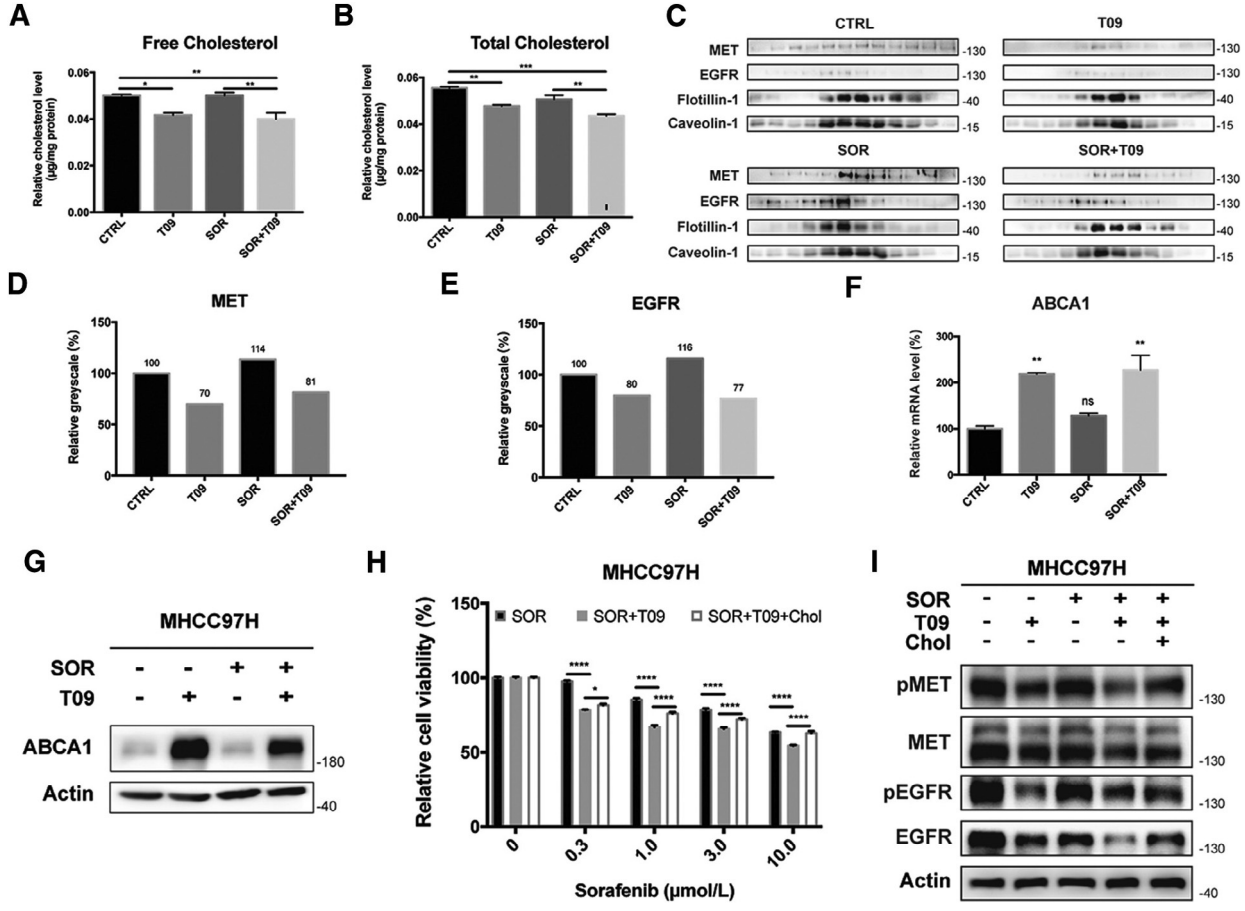

Fig. 4. T0901317 promotes cholesterol efflux by up-regulating ABCA1. (A-B) Quantification of free (A) and total (B) cytoplasmic cholesterol in MHCC97H cells after combination therapy. (C) Western blot analysis of MET and EGFR in lipid rafts in MHCC97H cells incubated in SOR with/without T09. (D-E) Quantification of MET (D) and EGFR (E) in lipid rafts in MHCC97H cells in (C). Expression level in CTRL group was standardized as 100%. (F-G) Quantitative real-time PCR (F) or western blot (G) of ABCA1 expression in MHCC97H cells after combination therapy. (H) Relative cell viabilities of MHCC97H cells treated by SOR, SOR with T09, and combination therapy with Cholesterol (Chol). (H) Effects of T09, SOR, and Chol on MET/EGFR pathways in MHCC97H cells. N 3, $^{*}P < .05$, $^{**}P < .01$, $^{***}P < .001$, $^{****}P < .0001$.

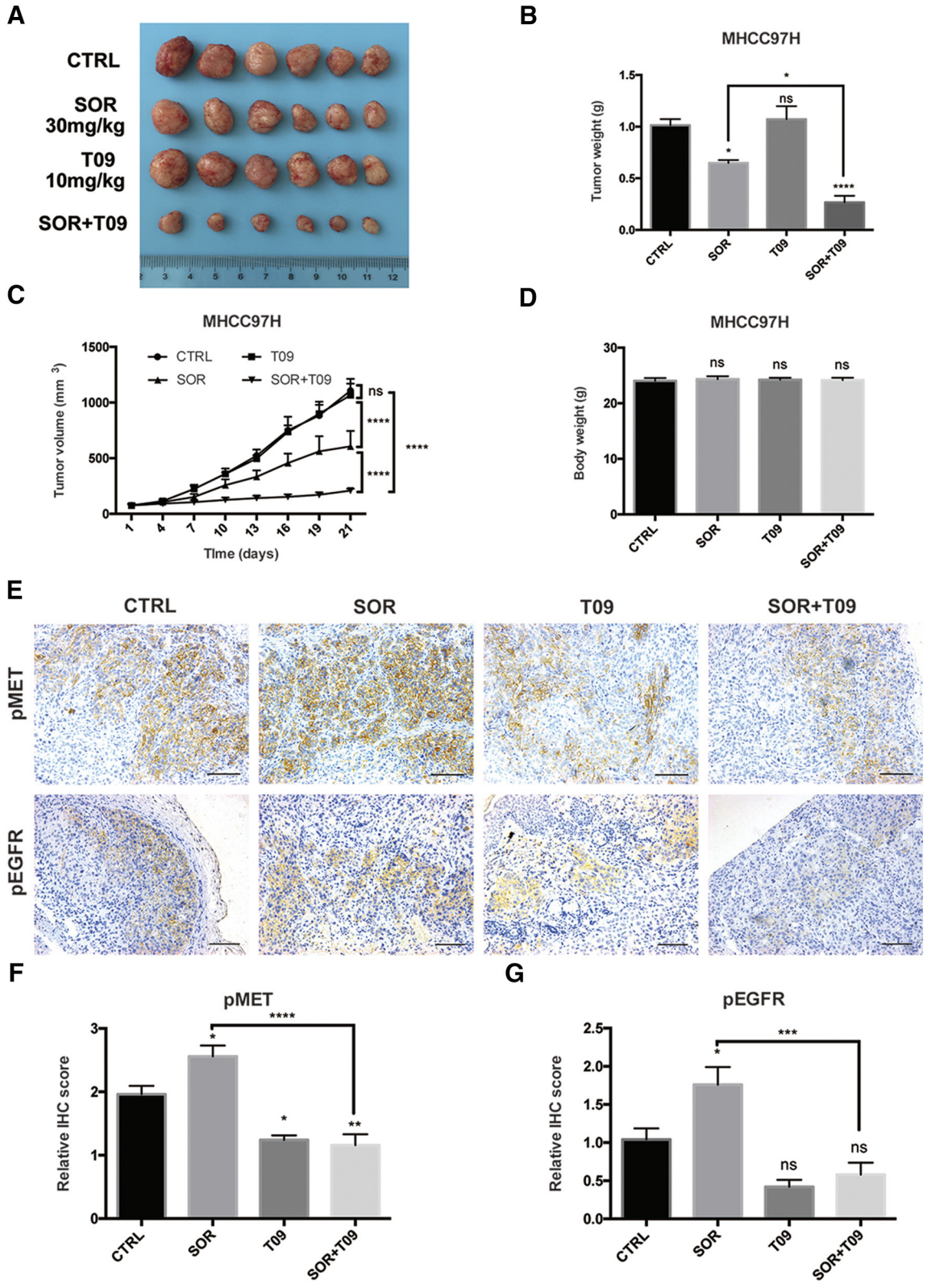

Fig. 5. T0901317 improves the efficacy of sorafenib *in vivo*. (A-B) Tumor volume (A) and tumor weight (B) in MHCC97H xenograft mouse model at day 21 (n = 6). (C) Tumor growth curves in mouse model after SOR and/or T09 treatment. (D) Body weight of the implantation mice at day 21. (E) Representative images of immunohistochemistry (IHC) staining for pMET and pEGFR from MHCC97H xenografts (200 magnification; scale bars, 100 m). (F-G) Quantitative analysis of IHC scores of pMET (F) and pEGFR (G) in each group in (E). N 3, $^{*}P < .05$, $^{**}P < .01$, $^{***}P < .001$, $^{****}P < .0001$.

activation of LXR increased triglyceride levels mainly through LXRα, while activating of LXRβ would not increase triglyceride production in the liver [35,36]. Given that increased liver and circulating triglyceride levels are the main side effects precluding further development of LXR agonists, selective activation of LXRβ is of great importance. GW3965 is a pan-agonist of LXR with a higher EC50 for LXRβ [37]. However, no significant differences between GW3965 and T0901317 were observed in their anti-proliferation effects in our set (Fig. S1*C*), which was consistent with other studies. One possible reason is that the working concentration of GW3965 is much higher than its EC50 value at both isoforms of LXR. Although we have drawn the conclusion that agonism of LXR can enhance sorafenib's efficacy in high LXR-β/α expression ratio population, applying LXRβ specific agonist will further strengthen it.

As is shown above, LXRβ expression was found to be up-regulated in HCC tumor tissues and correlated with high tumor grades and poor survival in TCGA samples (Fig. S3) [28]. Thus, we applied IHC analysis in clinical samples of 10 HCC patients to determine the correlation between LXRβ and MET or EGFR. However, no significant correlations were observed (data not shown). There are two possible reasons for this phenomenon, one is that LXRs can either be activated or inhibited by different ligands. Therefore, the expression levels of LXRs cannot fully reflect their roles in cancer progression. Another explanation is the heterogeneity of HCC. Due to the low positive incidence of LXRβ, MET and EGFR, it is reasonable to enlarge cases to determine the correlations.

We have observed that T0901317 with/without sorafenib dual inhibited MET and EGFR in whole cell lysates and lipid rafts (Fig. 3, *A–C* and Fig. 4, *C–E*), which is coordinated with our main conclusion, that is, T0901317 sensitizes HCC cells to sorafenib by dual-blockade of MET and EGFR. Another interesting phenomenon was that MET and EGFR in lipid rafts was up-regulated after sorafenib treatment (Fig. 4, *C–E*). Combining up-regulation of pMET and pEGFR in sorafenib group in mouse model (Fig. 5, *E–G*), we assume that exposure to sorafenib will recruit MET and EGFR in lipid rafts. Since lipid rafts play an important role in signal transduction of membrane receptors including RTKs [38–40], such recruitment by sorafenib is of great significance and requires further investigations.

In conclusion, our results provide new insights suggesting that cholesterol metabolism affects multiple RTKs and their downstream pathways. And targeting cholesterol metabolism improves sorafenib's efficacy in HCC. In addition, this study provides a mechanism-based rationale for the action of targeting cholesterol metabolism in cancer treatment. However, there are still a number of fundamental questions that remain to be answered. Are there other RTKs that response to LXR-cholesterol axis, and do they correlate with sorafenib's efficacy? Whether statins or other interventions targeting cholesterol metabolism exhibit similar effects? Does cholesterol metabolism play a central role in regulating the efficacy of other TKIs? All the above questions require further investigations.

Conflict of interest

The authors declare no conflicts of interest.

Acknowledgements

We thank Dr. Kaili Zhang for the support in cholesterol assay. We also thank Dr. Yanfeng Liu, Dr. Jing Yang for their assistance in the xenograft mouse model.

Funding

This work was supported by the National Science and Technology Major Project of the thirteenth Five-Year Plan (grant number 2017ZX10203207); the Natural Science Foundation of China (grant number 81472677; Shanghai Rising-Star Program (grant number 17QA140070).

Appendix A. Supplementary data

Supplementary data to this article can be found online at https://doi.org/10.1016/j.neo.2019.08.002.

References

1. Bray F, Ferlay J, Soerjomataram I, Siegel RL, Torre LA, Jemal A, etal. Global cancer statistics 2018: GLOBOCAN estimates of incidence and mortality worldwide for 36 cancers in 185 countries. *CA Cancer J Clin* 2018;**68**:394–424.
2. Llovet JM, Ricci S, Mazzaferro V, Hilgard P, Gane E, Blanc JF, etal. Sorafenib in advanced hepatocellular carcinoma. *N Engl J Med* 2008;**359**:378–90.
3. Cheng AL, Kang YK, Chen Z, Tsao CJ, Qin S, Kim JS, etal. Efficacy and safety of sorafenib in patients in the Asia-Pacific region with advanced hepatocellular carcinoma: a phase III randomised, double-blind, placebo-controlled trial. *Lancet Oncol* 2009;**10**:25–34.
4. Chen KF, Chen HL, Tai WT, Feng WC, Hsu CH, Chen PJ, etal. Activation of phosphatidylinositol 3-kinase/Akt signaling pathway mediates acquired resistance to sorafenib in hepatocellular carcinoma cells. *J Pharmacol Exp Ther* 2011;**337**:155–61.
5. Rudalska R, Dauch D, Longerich T, McJunkin K, Wuestefeld T, Kang TW, etal. In vivo RNAi screening identifies a mechanism of sorafenib resistance in liver cancer. *Nat Med* 2014;**20**:1138–46.
6. Chen HA, Kuo TC, Tseng CF, Ma JT, Yang ST, Yen CJ, etal. Angiopoietin-like protein 1 antagonizes MET receptor activity to repress sorafenib resistance and cancer stemness in hepatocellular carcinoma. *Hepatology* 2016;**64**:1637–51.
7. Firtina Karagonlar Z, Koc D, Iscan E, Erdal E, Atabey N. Elevated hepatocyte growth factor expression as an autocrine c-Met activation mechanism in acquired resistance to sorafenib in hepatocellular carcinoma cells. *Cancer Sci* 2016;**107**:407–16.
8. Han P, Li H, Jiang X, Zhai B, Tan G, Zhao D, etal. Dual inhibition of Akt and c-Met as a second-line therapy following acquired resistance to sorafenib in hepatocellular carcinoma cells. *Mol Oncol* 2017;**11**:320–34.
9. Dong XF, Liu TQ, Zhi XT, Zou J, Zhong JT, Li T, etal. COX-2/PGE2 axis regulates HIF-2alpha activity to promote hepatocellular carcinoma hypoxic response and reduce the sensitivity of sorafenib treatment. *Clin Cancer Res* 2018;**24**:3204–16.
10. Yoon S, Lee EJ, Choi JH, Chung T, Kim DY, Im JY, etal. Recapitulation of pharmacogenomic data reveals that invalidation of SULF2 enhance sorafenib susceptibility in liver cancer. *Oncogene* 2018;**37**:4443–54.
11. Ding C, Zhang C, Zhang M, Chen YZ, Tan C, Tan Y, etal. Multitarget inhibitors derived from crosstalk mechanism involving VEGFR2. *Future Med Chem* 2014;**6**:1771–89.
12. Lin CY, Gustafsson JA. Targeting liver X receptors in cancer therapeutics. *Nat Rev Cancer* 2015;**15**:216–24.
13. Lo Sasso G, Bovenga F, Murzilli S, Salvatore L, Di Tullio G, Martelli N, etal. Liver X receptors inhibit proliferation of human colorectal cancer cells and growth of intestinal tumors in mice. *Gastroenterology* 2013;**144**:1497–507.
14. Hu C, Liu D, Zhang Y, Lou G, Huang G, Chen B, etal. LXRalpha-mediated downregulation of FOXM1 suppresses the proliferation of hepatocellular carcinoma cells. *Oncogene* 2014;**33**:2888–97.
15. Pencheva N, Buss CG, Posada J, Merghoub T, Tavazoie SF. Broad-spectrum therapeutic suppression of metastatic melanoma through nuclear hormone receptor activation. *Cell* 2014;**156**:986–1001.
16. Alioui A, Dufour J, Leoni V, Loregger A, Moeton M, Iuliano L, etal. Liver X receptors constrain tumor development and metastasis dissemination in PTEN-deficient prostate cancer. *Nat Commun* 2017;**8**:445.
17. Tavazoie MF, Pollack I, Tanqueco R, Ostendorf BN, Reis BS, Gonsalves FC, etal. LXR/ApoE activation restricts innate immune suppression in cancer. *Cell* 2018;**172**:825–40.

18. Guo D, Reinitz F, Youssef M, Hong C, Nathanson D, Akhavan D, etal. An LXR agonist promotes glioblastoma cell death through inhibition of an EGFR/AKT/SREBP-1/LDLR-dependent pathway. *Cancer Discov* 2011;**1**:442–56.
19. Noghero A, Perino A, Seano G, Saglio E, Lo Sasso G, Veglio F, etal. Liver X receptor activation reduces angiogenesis by impairing lipid raft localization and signaling of vascular endothelial growth factor receptor-2. *Arterioscler Thromb Vasc Biol* 2012;**32**:2280–8.
20. Pommier AJ, Alves G, Viennois E, Bernard S, Communal Y, Sion B, etal. Liver X receptor activation downregulates AKT survival signaling in lipid rafts and induces apoptosis of prostate cancer cells. *Oncogene* 2010;**29**:2712–23.
21. Wang B, Tontonoz P. Liver X receptors in lipid signalling and membrane homeostasis. *Nat. Rev. Endocrinol.* 2018;**14**:452–63.
22. Villa GR, Hulce JJ, Zanca C, Bi J, Ikegami S, Cahill GL, etal. An LXR-cholesterol axis creates a metabolic co-dependency for brain cancers. *Cancer Cell* 2016;**30**:683–93.
23. Bovenga F, Sabba C, Moschetta A. Uncoupling nuclear receptor LXR and cholesterol metabolism in cancer. *Cell Metab* 2015;**21**:517–26.
24. Hong C, Tontonoz P. Liver X receptors in lipid metabolism: opportunities for drug discovery. *Nat. Rev. Drug Discov* 2014;**13**:433–44.
25. Jakobsson T, Treuter E, Gustafsson JA, Steffensen KR. Liver X receptor biology and pharmacology: new pathways, challenges and opportunities. *Trends Pharmacol Sci* 2012;**33**:394–404.
26. Chou TC. Drug combination studies and their synergy quantification using the Chou-Talalay method. *Cancer Res* 2010;**70**:440–6.
27. Calkin AC, Tontonoz P. Liver x receptor signaling pathways and atherosclerosis. *Arterioscler Thromb Vasc Biol* 2010;**30**:1513–8.
28. Chandrashekar DS, Bashel B, Balasubramanya SAH, Creighton CJ, Ponce-Rodriguez I, Chakravarthi BVSK, etal. UALCAN: a portal for facilitating tumor subgroup gene expression and survival analyses. *Neoplasia* 2017;**19**:649–58.
29. Kim KH, Lee GY, Kim JI, Ham M, Won Lee J, Kim JB. Inhibitory effect of LXR activation on cell proliferation and cell cycle progression through lipogenic activity. *J Lipid Res* 2010;**51**:3425–33.
30. Galmiche A, Chauffert B, Barbare JC. New biological perspectives for the improvement of the efficacy of sorafenib in hepatocellular carcinoma. *Cancer Lett* 2014;**346**:159–62.
31. Chen J, Jin R, Zhao J, Liu J, Ying H, Yan H, etal. Potential molecular, cellular and microenvironmental mechanism of sorafenib resistance in hepatocellular carcinoma. *Cancer Lett* 2015;**367**:1–11.
32. Lu M, Hu XH, Li Q, Xiong Y, Hu GJ, Xu JJ, etal. A specific cholesterol metabolic pathway is established in a subset of HCCs for tumor growth. *J Mol Cell Biol* 2013;**5**:404–15.
33. Fang Z, Jung KH, Yan HH, Kim SJ, Rumman M, Park JH, etal. Melatonin synergizes with sorafenib to suppress pancreatic cancer via melatonin receptor and PDGFR-β/STAT3 pathway. *Cell Physiol Biochem* 2018;**47**:1751–68.
34. Hozoji-Inada M, Munehira Y, Nagao K, Kioka N, Ueda K. Liver X receptor beta (LXRbeta) interacts directly with ATP-binding cassette A1 (ABCA1) to promote high density lipoprotein formation during acute cholesterol accumulation. *J Biol Chem* 2011;**286**:20117–24.
35. Bensinger SJ, Tontonoz P. Integration of metabolism and inflammation by lipid-activated nuclear receptors. *Nature* 2008;**454**:470–7.
36. Bradley MN, Hong C, Chen M, Joseph SB, Wilpitz DC, Wang X, etal. Ligand activation of LXR β reverses atherosclerosis and cellular cholesterol overload in mice lacking LXR a and apoE. *J Clin Invest* 2007;**117**:2337–46.
37. Collins JL, Fivush AM, Watson MA, Galardi CM, Lewis MC, Moore LB, etal. Identification of a nonsteroidal liver X receptor agonist through parallel array synthesis of tertiary amines. *J Med Chem* 2002;**45**:1963–6.
38. Cairns RA, Harris IS, Mak TW. Regulation of cancer cell metabolism. *Nat Rev Cancer* 2011;**11**:85–95.
39. Zhuang L, Kim J, Adam RM, Solomon KR, Freeman MR. Cholesterol targeting alters lipid raft composition and cell survival in prostate cancer cells and xenografts. *J Clin Invest* 2005;**115**:959–68.
40. Adachi S, Nagao T, Ingolfsson HI, Maxfield FR, Andersen OS, Kopelovich L, etal. The inhibitory effect of ()-epigallocatechin gallate on activation of the epidermal growth factor receptor is associated with altered lipid order in HT29 colon cancer cells. *Cancer Res* 2007;**67**:6493–501.